structural communications

Structure of *Escherichia coli* aspartate α-decarboxylase Asn72Ala: probing the role of Asn72 in pyruvoyl cofactor formation

**Michael E. Webb,[a]*‡
Carina M. C. Lobley,[b]§ Fatima
Soliman,[b]¶ Mairi L. Kilkenny,[b]
Alison G. Smith,[c] Tom L.
Blundell[b] and Chris Abell[a]**

[a]University Chemical Laboratory,
University of Cambridge, Lensfield Road,
Cambridge CB2 1EW, England, [b]Department of
Biochemistry, University of Cambridge, Tennis
Court Road, Cambridge CB2 1QW, England,
and [c]Department of Plant Sciences,
University of Cambridge, Downing Street,
Cambridge CB2 3EA, England

‡ Present address: School of Chemistry and
Astbury Centre for Structural Molecular Biology,
University of Leeds, Woodhouse Lane,
Leeds LS2 9JT, England.
§ Present address: Diamond Light Source,
Harwell Science and Innovation Campus,
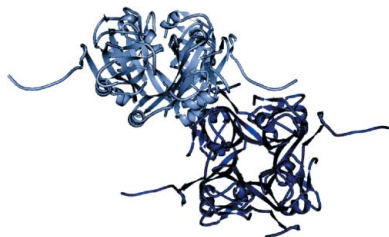Didcot, Oxfordshire OX11 0DE, England.
¶ Present address: Sackler Institute for
Developmental Psychobiology, Weill Medical
Institute at Cornell University, 1300 York
Avenue, NY 10021, USA.

Correspondence e-mail: m.e.webb@leeds.ac.uk

The crystal structure of the Asn72Ala site-directed mutant of *Escherichia coli* aspartate α-decarboxylase (ADC) has been determined at 1.7 Å resolution. The refined structure is consistent with the presence of a hydrolysis product serine in the active site in place of the pyruvoyl group required for catalysis, which suggests that the role of Asn72 is to protect the ester formed during ADC activation from hydrolysis. In previously determined structures of activated ADC, including the wild type and other site-directed mutants, the C-terminal region of the protein is disordered, but in the Asn72Ala mutant these residues are ordered owing to an interaction with the active site of the neighbouring symmetry-related multimer.

1. Introduction

Aspartate α-decarboxylase (ADC) catalyses the formation of β-alanine in the bacterial pantothenate-biosynthesis pathway (Webb *et al.*, 2004). This enzyme is a member of a small class of pyruvoyl-dependent decarboxylases in which the enzyme-bound pyruvoyl cofactor is generated *via* the autocatalytic rearrangement of a serine residue *via* an ester intermediate (van Poelje & Snell, 1990). ADC is the prototypical member of the double-ψ β-barrel superfamily (Castillo *et al.*, 1999) and crystal structures of processed apo ADC and the ester intermediate during activation (PDB entry 1aw8; Albert *et al.*, 1998) have been reported, as have crystal structures of seven site-directed mutants of the enzyme in a variety of activation states together with that of the unprocessed zymogen (PDB entry 1ppy; Schmitzberger *et al.*, 2003). The crystal structure of the *Helicobacter pylori* protein bound to a substrate analogue has also been determined (Lee & Suh, 2004), as has the structure of the uncleaved protein from *Mycobacterium tuberculosis* (Gopalan *et al.*, 2006). Structures of the activated enzyme from *Thermus thermophilus* (PDB entry 1vc3; RIKEN Structural Genomics/Proteomics Initiative, unpublished work), *Francisella tularensis* (PDB entry 3oug; Center for Structural Genomics of Infectious Diseases, unpublished work) and *Campylobacter jejuni* (PDB entry 3plx; Center for Structural Genomics of Infectious Diseases, unpublished work) have also been reported. In ADC, the pyruvoyl group is generated *via* a rearrangement of Ser25 and cleavage of the unprocessed π-chain to generate a β-chain (residues 1–24) and an α-chain (residues 25–126) with an N-terminal pyruvoyl group (Ramjee *et al.*, 1997). An alternative product, the α′-chain, in which hydrolysis has occurred to generate an N-terminal serine, is also observed. In crystal structures of the unprocessed enzyme, the main chain of residues 20–24 can easily be fitted into the electron density. However, after activation the electron density for this region is weak, highlighting the conformational flexibility resulting from cleavage of the protein backbone. In all of the previously determined crystal structures there is insufficient electron density to model the C-terminal ten residues of the α-chain. The site-directed mutant Gly24Ser is the exception to this rule, with only the last four residues unmodelled. In this study, we report the crystal structure of the site-directed mutant Asn72Ala. Asn72 is

Table 1
Data-collection and refinement statistics.

Values in parentheses are for the outermost shell.

Data collection	
X-ray source	SRS beamline 14.2
Wavelength (Å)	0.9871
Space group	$P6_122$
Unit-cell parameters (Å, °)	$a = 71.1$, $b = 71.1$, $c = 215.8$, $\alpha = \beta = 90$, $\gamma = 120$
Resolution (Å)	30–1.7 (1.73–1.70)
R_{merge}	0.043 (0.288)
$\langle I/\sigma(I)\rangle$	59.3 (9.3)
Completeness (%)	99.9 (100)
Multiplicity	11.75
Refinement	
No. of reflections	430834
No. of unique reflections	36655 (2507)
R_{cryst}	0.165 (0.171)
R_{free}	0.185 (0.178)
Mosaicity (°)	0.21
No. of atoms	
Protein	1859
Ligand	10
Water	225
Average B factors (Å²)	
Protein	18.6
Sulfate	32.8
Waters	34.4
R.m.s. deviations	
Bond lengths (Å)	0.011
Bond angles (°)	1.286
Ramachandran statistics (%)	
Most favoured	98
Generously allowed	2
Disallowed	0
PDB code	3tm7

hydrogen bonded to the β-hydroxyl group of Ser25 in the unprocessed structure of ADC, holding this residue in an unreactive conformation; the structure was therefore expected to reveal the conformation of the peptide backbone prior to the autocatalytic cleavage reaction.

2. Materials and methods

2.1. Generation of the Asn72Ala site-directed mutant

The Asn72Ala mutant was generated *via* site-directed mutagenesis. The following oligonucleotides were used: 5′-CGAGAATTATTTC-TGTTGCCGGTGCGGCGG-3′ and 5′-CCGCCGCACCGGCAAC-AGAAATAATTCTCG-3′. The QuikChange method (Stratagene) was used with *Escherichia coli panD* subcloned into the expression vector pRSETA as a template. The recombinant protein was over-expressed in *E. coli* C41 (DE3) and purified to homogeneity as described elsewhere (Schmitzberger *et al.*, 2003). Protein mass spectra were obtained *via* MALDI–TOF analysis as described elsewhere (Webb *et al.*, 2003).

2.2. Crystallization, data collection and processing

The protein was concentrated *via* centrifugal concentration to a final concentration of 19 mg ml^{-1} in 50 m*M* Tris–HCl pH 8.0. Protein crystals were grown using the hanging-drop method at 292 K. Drops consisted of 1 µl protein solution and 1 µl 1.6 *M* ammonium sulfate pH 4.0, and the reservoir contained 500 µl 1.6 *M* ammonium sulfate pH 4.0. Hexagonal bipyrimidal crystals appeared within 3 d. Crystals were cryoprotected in 1.8 *M* ammonium sulfate, 0.1 *M* citric acid, 30% glycerol pH 4.0 using 5% increments in glycerol concentration to prevent crystal dissolution. A complete data set was obtained from

a single crystal at 100 K. Diffraction data were collected to 1.7 Å maximum resolution on beamline 14.2 at the Synchrotron Radiation Source (Daresbury) using an ADSC Q4 CCD. Data were indexed and integrated using *DENZO* v.1.97.2 and scaled with *SCALEPACK* v.1.97.2 (Otwinowski & Minor, 1997). Data conversion into structure-factor amplitudes and all further data manipulations were performed using the *CCP*4 suite v.4.2.1 (Winn *et al.*, 2011). The associated statistics are shown in Table 1.

2.3. Crystal structure refinement

The wild-type ADC model was used for structure solution by molecular replacement with *AMoRe* (Navaza, 2001). The first 17 residues (residues 20–26), which are highly disordered, and the C-terminus (residue 115–126) were initially omitted from refinement and were later built in manually. A random test set consisting of 5% of the reflections was assigned as the free reflection set and refinement using *REFMAC* v.5.1.24 (Murshudov *et al.*, 2011) and manual rebuilding using *XtalView* were iterated until the values of R_{cryst} and R_{free} converged (Table 1).
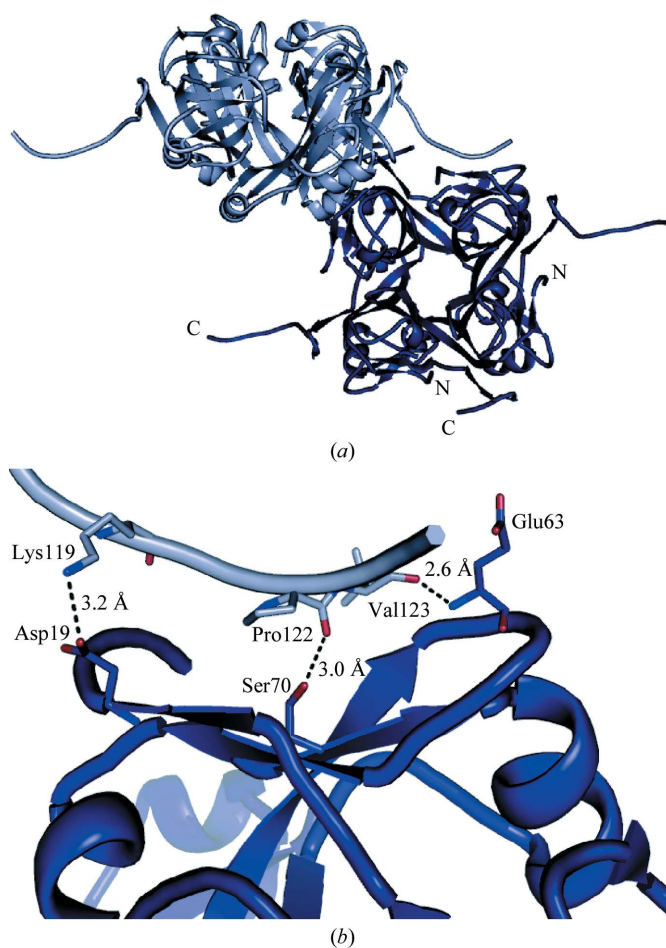

(a)

(b)

Figure 1
(a) Interaction of symmetry-related protomers in the crystal packing of the ADC Asn72Ala site-directed mutant. The C-terminal portion of protomer *B* (light grey) interacts with the the activation-site region of a neighbouring symmetry-related protomer (dark blue). The N- and C-termini of the protomers in one asymmetric unit are labelled. (b) Hydrogen-bonding interactions occur between the carbonyl of Pro122 and the side chain of Ser70 and between the carbonyl of Val123 and the amide of Glu63. A charge–charge interaction between Lys119 and Asp19 is also observed.

3. Results and discussion

3.1. Crystal structure of ADC Asn72Ala

The final model of ADC Asn72Ala was refined in the resolution range 30.0–1.7 Å to a crystallographic R value of 16.0%. The protein crystallized in space group $P6_122$, with two protomers of the native tetramer per asymmetric unit. In protomer A the N-terminal His tag and C-terminal residues 119–126 were not modelled owing to poor electron density, whereas in protomer B the electron density was of sufficient quality to rebuild the structure as far as residue 125. In the previously refined structure of the ADC Gly24Ser mutant the model only extended to residue Pro122; in other structures this region was wholly unmodelled. The C-terminal region appears to interact non-covalently with a symmetry-related protomer B as a result of crystal packing (see Fig. 1a). The nature of these interactions and their physiological significance is discussed further below.

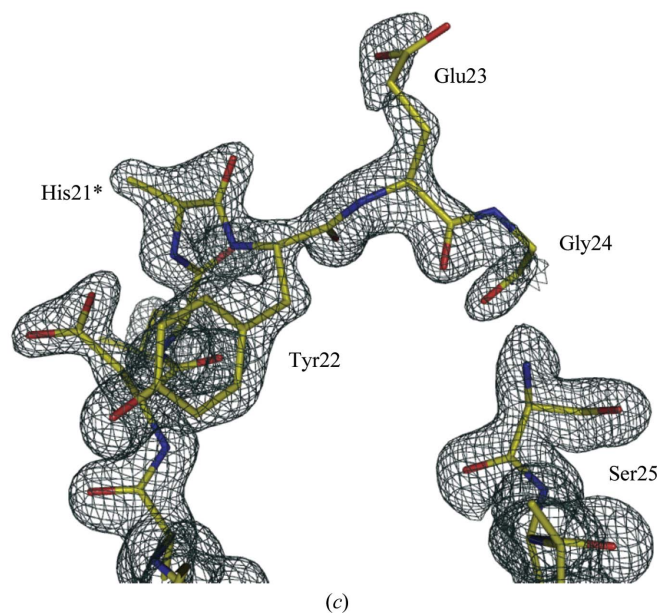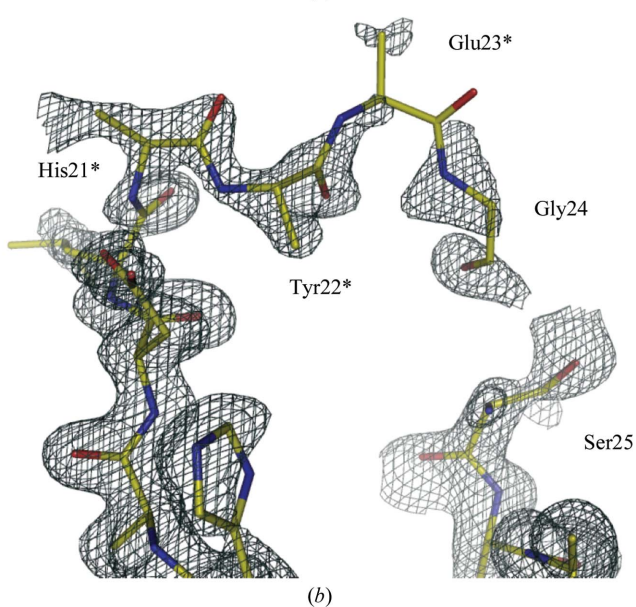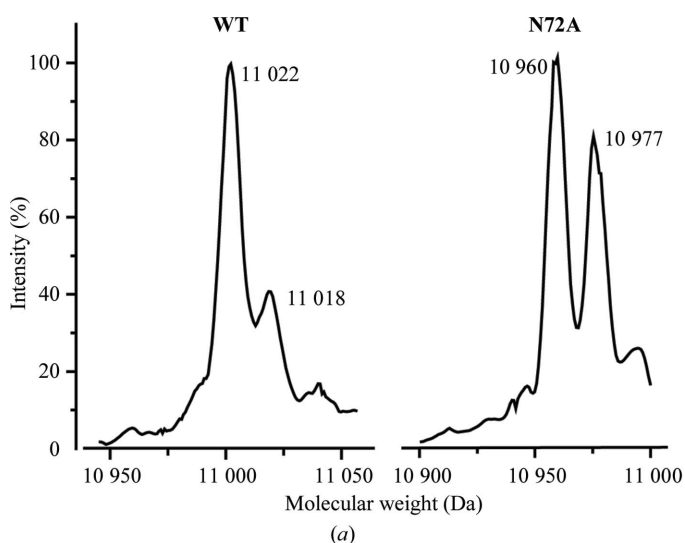### 3.2. Activation state of ADC Asn72Ala

The structure of the ADC Asn72Ala mutant was determined in order to identify the relative importance of the hydrogen bond formed between the β-amide of Asn72 and the β-hydroxyl group of Ser25. The serine functional group carries out a nucleophilic attack on the main-chain carbonyl of Gly24 in the first step of the auto-catalytic activation reaction (Ramjee *et al.*, 1997) to form two shorter α- and β-chains from the zymogenic π-chain, leaving a pyruvoyl group at the N-terminal end of the α-chain. The crystal structure of the unreacted zymogen (Schmitzberger *et al.*, 2003) revealed the presence of a hydrogen bond between the β-hydroxyl of Ser25 and the side-chain amide of Asn72 which held Ser25 in an unreactive conformation; the hydroxyl group is held in the plane of the carbonyl group which it attacks, and mutation to alanine might therefore be expected to lead to an increased observed rate of activation. Somewhat surprisingly, this was not the case and the rate of activation (as measured by Tris–Tricine gel electrophoresis; not shown) was similar to that of wild-type protein. However, mass-spectrometric analysis of the product chain produced at pH 7 indicated that a larger proportion of the α'-chain hydrolysis product in which a serine residue is present at the N-terminus is formed (see Fig. 2a). The electron density in the active site of the Asn72Ala mutant is consistent with this observation; while chain cleavage has occurred, the electron density can be readily fitted with a serine residue but there is no evidence for the presence of a pyruvoyl group (Figs. 2b and 2c). It is presumed that the rate of specific base-catalysed hydrolysis of the ester intermediate during activation will be enhanced at the lower pH at which the crystals were grown. These observations suggest that residue Asn72, rather than being involved in the first step of the activation reaction, in fact protects the ester intermediate from solvent-mediated hydrolysis by hindering the approach of water to the face of the ester.

Figure 2
(a) MALDI–TOF MS analysis of the ADC Asn72Ala activation state. An elevated proportion of the α'-chain hydrolysis product is observed (10 977 Da) compared with wild-type ADC. (b, c) Electron density of the two protomers in the asymmetric unit. In both protomers the observed electron density is consistent with the presence of a serine residue at position 25. (b) In protomer A, residues 21–24 are poorly resolved and residues 21–23 are modelled as alanine residues. (c) In protomer B, the side chains of residues 21–23 can be modelled into electron density; this is owing to interactions between these residues and the C-terminus of a neighbouring symmetry-related protomer in the crystal.

3.3. Interactions between symmetry-related protomers

As stated above, the C-terminus of protomer *B* is well resolved in this structure as a result of noncovalent interactions between the C-terminus and the activation site of a symmetry-related protomer. Hydrogen bonds or electrostatic interactions between the carbonyl of Lys119 and the amide N atom of Glu23, between the ε-amino group of Lys119 and the β-carboxylate of Asp9, between the carbonyl of Pro122 and the β-hydroxy group of Ser70, between the carbonyl of Val123 and the amide of Glu63 and between the amide of Ala125 and the γ-carboxylate of Glu63 appear to contribute to this interaction (Fig. 1*b*). Additionally, the side chains of Ile121 and Pro122 are packed against the side chains of Ala62 and Tyr22, respectively. The specific nature of this interaction would suggest that it may have some physiological significance; however, three observations suggest that this is unlikely. The C-terminal carboxylate is 3.54 Å from the side chain of Glu113 in the symmetry-related protomer, suggesting that a hydrogen bond occurs between these groups; at physiological pH it is anticipated that both functional groups would be deprotonated, preventing this interaction between the two proteins. Secondly, it is probable that a number of the observed interactions are only possible as a result of the mutation. In the wild-type zymogen structure the β-hydroxyl group of Ser70 is hydrogen bonded to the side-chain amide of Asn72; it is therefore not able to interact with the carbonyl of Pro122. Also, if the deleted side chain of Asn72 is modelled back into the structure then a steric clash between this side chain and the side chain of Ile121 is generated. These observations suggest that the interaction between the C-terminus and the active site of another ADC molecule does not have any physiological significance but is purely an artefact of crystallographic packing.

4. Conclusion

We have investigated the function of residue Asn72 in the activation of aspartate α-decarboxylase to generate a pyruvoyl group. This residue is not required for activation of the protein; however, it may protect the ester intermediate in activation from hydrolysis. Surprisingly, we observed interactions between symmetry-related multimers in the crystal structure mediated *via* three specific interactions. These interactions are precluded in the wild-type structure, suggesting that they are not physiologically significant.

References

Albert, A., Dhanaraj, V., Genschel, U., Khan, G., Ramjee, M. K., Pulido, R., Sibanda, B. L., von Delft, F., Witty, M., Blundell, T. L., Smith, A. G. & Abell, C. (1998). *Nature Struct. Biol.* **5**, 289–293.

Castillo, R. M., Mizuguchi, K., Dhanaraj, V., Albert, A., Blundell, T. L. & Murzin, A. G. (1999). *Structure*, **7**, 227–236.

Gopalan, G., Chopra, S., Ranganathan, A. & Swaminathan, K. (2006). *Proteins*, **65**, 796–802.

Lee, B. I. & Suh, S. W. (2004). *J. Mol. Biol.* **340**, 1–7.

Murshudov, G. N., Skubák, P., Lebedev, A. A., Pannu, N. S., Steiner, R. A., Nicholls, R. A., Winn, M. D., Long, F. & Vagin, A. A. (2011). *Acta Cryst.* D**67**, 355–367.

Navaza, J. (2001). *Acta Cryst.* D**57**, 1367–1372.

Otwinowski, Z. & Minor, W. (1997). *Methods Enzymol.* **276**, 301–326.

Poelje, P. D. van & Snell, E. E. (1990). *Annu. Rev. Biochem.* **59**, 29–59.

Ramjee, M. K., Genschel, U., Abell, C. & Smith, A. G. (1997). *Biochem. J.* **323**, 661–669.

Schmitzberger, F., Kilkenny, M. L., Lobley, C. M., Webb, M. E., Vinkovic, M., Matak-Vinkovic, D., Witty, M., Chirgadze, D. Y., Smith, A. G., Abell, C. & Blundell, T. L. (2003). *EMBO J.* **22**, 6193–6204.

Webb, M. E., Smith, A. G. & Abell, C. (2004). *Nat. Prod. Rep.* **21**, 695–721.

Webb, M. E., Stephens, E. G., Smith, A. G. & Abell, C. (2003). *Chem. Commun.*, pp. 2416–2417.

Winn, M. D. *et al.* (2011). *Acta Cryst.* D**67**, 235–242.